



How to define energy function for memristive oscillator and map

Yitong Guo · Ying Xie · Jun Ma 

Received: 29 July 2023 / Accepted: 15 October 2023 / Published online: 2 November 2023
© The Author(s), under exclusive licence to Springer Nature B.V. 2023

Abstract During the release and propagation of intracellular and extracellular ions, electromagnetic field is induced accompanying with propagation of energy flow. The firing mode is dependent on the energy level, and external energy injection will induce distinct mode transition. Exact energy function for a neuron developed from a neural circuit can be obtained directly by applying scale transformation for the physical field energy. For generic neuron models, dimensionless Hamilton energy function can be obtained by using Helmholtz theorem, and this energy function can be considered as a specific Lyapunov function. In this review, approach of energy function for memristive neuron is discussed by designing equivalent neural circuit coupled by two kinds of memristors, which are dependent on the magnetic flux and charge flux, respectively. A scheme is suggested to get equivalent energy function for memristive neuron in the form of map by

introducing a scale parameter. The memristive map reduced from the memristive neuron can produce similar attractors and firing modes under applying the same parameters, and the average Hamilton energy for the map neuron is decreased because of regulation from the scale parameter. On the other hand, a memristive map is replaced by an equivalent memristive oscillator for finding an equivalent Hamilton energy function according to the Helmholtz theorem. The energy scheme can be helpful for further investigating energy property of artificial neurons, maps and discrete memristors. It also provides evidence that maps are more suitable for investigating neural activities than neuron oscillators.

Keywords Hamilton energy · Memristive neuron · Neural circuit · Memristor

Y. Guo · J. Ma (✉)
College of Electrical and Information Engineering,
Lanzhou University of Technology, Lanzhou 730050,
China
e-mail: hyperchaos@163.com

Y. Guo · J. Ma
Department of Physics, Lanzhou University of
Technology, Lanzhou 730050, China

Y. Xie · J. Ma
School of Science, Chongqing University of Posts and
Telecommunications, Chongqing 430065, China

1 Introduction

The occurrence of chaos and chaos in nonlinear circuits depends on the involvement of electric components, and one nonlinear component with nonlinear relation between voltage and channel current is required at least. When these circuits are activated, capacitive energy is shunted to inductive channels and memristive channels based on memristors [1–5]. A simple nonlinear circuit requires the

combination and connection to capacitor, inductor, negative resistor and even external signal source, and appropriate setting in parameters will develop chaos in these nonlinear circuits [6–10]. In particular, some nonlinear circuits can be tamed and improved to present bursting, spiking patterns, and neural circuits are obtained to propose equivalent neuron models. Indeed, piezoelectric ceramic [11], Josephson junction [12, 13], photocell [14, 15], thermistor [16, 17], memristor can be connected to some neural circuits for building reliable neural circuits for further considering the physical effect during activating neural activities in biophysical neurons [18–22].

From physical aspect, energy is exchanged and propagated when biological neurons present different firing modes and patterns. For nonlinear circuits, continuous oscillation needs stable energy supply and shunting between different electric components. The physical energy in nonlinear circuits can be obtained by considering the energy in the capacitive, inductive and memristive channels, and then the physical field energy can be converted into equivalent dimensionless energy function [23–25] by applying scale transformation on the variables and parameters in the field energy function. On the other hand, suitable Hamilton energy function can be confirmed in a nonlinear oscillator by using Helmholtz theorem [26–28]. However, it keeps open for discrete systems and maps to get energy function, and the involvement of discrete memristor makes the question become more interesting and worthy of investigation.

In this review, based on a memristive map [29, 30], a scheme is used to estimate the energy function in theoretical way. A scale parameter is introduced to build a equivalent continuous dynamical system for getting the Hamilton energy function and then the value for the scale parameter is confirmed by bifurcation analysis, which the memristive map has the same maximal value or phase space with the memristive oscillator. This scheme can be further used to calculate energy for more maps and energy level will be switched to control the chaos in maps.

2 Energy in nonlinear circuit and continuous oscillator

Quiescent biological neurons develop static distribution of electric field, and the membrane potential keeps

certain constants for keeping propagation balance of intracellular and extracellular ions. In presence of external stimulus beyond the threshold, certain firing mode is triggered to present continuous firing patterns accompanying with jumping between energy levels. That is, distinct physical effect becomes distinct and it can be reproduced in some equivalent neural circuits by considering the main physical properties. The capacitive energy can be described by the capacitors and charge-controlled memristor [31–34], the inductive energy can be mimicked by inductors and magnetic-flux dependent memristor [35–38], nonlinear resistor in parallel with the inductive channel can be used to bridge connection to the magnetic field and electric field. In addition, involvement of constant voltage sources into the inductive channel or memristive channel is suitable to represent the resting potentials of ion channels. Biological neurons can induce electrical field and magnetic field, and ion channels are important for exchange and propagation of ions including calcium, potassium and sodium. Therefore, a capacitor and its output voltage are used to mimic the electric field and membrane potential, inductor and its channel current can describe the magnetic field and the transmembrane current. Additive memristors are used to estimate the physical field effect and special property of ion channels, such as detecting external field and self-adaption and controllability. In Fig. 1, a simple neural circuit is built by connecting one capacitor, two different kinds of memristors, one nonlinear resistor with cubic relation between channel current and across voltage, and

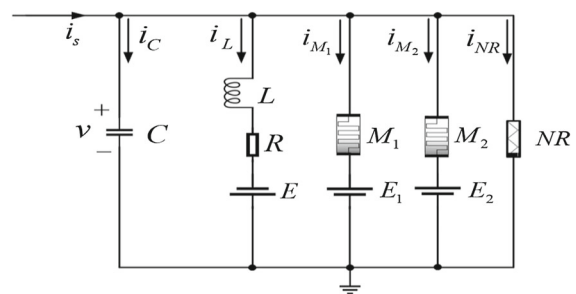


Fig. 1 Memristive neural circuit coupled by memristors. C , L , M_1 , M_2 , and NR describe capacitor, inductor, magnetic flux-dependent memristor, charge-controlled memristor, nonlinear resistor, respectively. Constant E denotes reverse potential, i_s represents external forcing current, the output voltage for capacitor is v

external stimulus can be time-varying or sampled from specific signal source within specific frequency band.

In Fig. 1, three different constant voltage sources are introduced to mimic the effect of reverse voltage in these ion channels. The involvement of NR is used to describe the nonlinear relation of energy flow between capacitive and inductive field. The channel current across the two memristors and nonlinear resistor is respectively estimated,

$$\begin{cases} i_{NR} = -\frac{1}{\rho} \left(v - \frac{1}{2} \frac{v^2}{V_0} - \frac{1}{3} \frac{v^3}{V_0^2} \right); \\ i_{M1} = M(\varphi)(v - E_1) = (a + 3b\varphi^2)(v - E_1); \\ i_{M2} = \frac{(v - E_2)}{W(q)} = (c + dq^2)(v - E_2); \end{cases} \quad (1)$$

where the physical parameters $(\rho, V_0), (a, b), (c, d)$ are relative to the material properties of the NR, M_1 and M_2 , respectively. The parameters (ρ, V_0) can be discerned from the i - v (current and voltage across the nonlinear resistor) curve when the nonlinear resistor is connected to a simple circuit. φ and q describe the magnetic flux and charges across the two kinds of memristors. v and i_L measure the voltage across the capacitor and channel current across the inductor. Furthermore, the field energy in each electric component, and the total energy function are respectively calculated by

$$\begin{cases} W_C = \frac{1}{2} C v^2; \quad W_L = \frac{1}{2} L i_L^2; \\ W_{M1} = \frac{1}{2} L_M i_{M1}^2 = \frac{1}{2} \varphi i_{M1} = \frac{1}{2} (a + 3b\varphi^2)(v - E_1)\varphi; \\ W_{M2} = \frac{1}{2} C_M v_{M2}^2 = \frac{1}{2} q v_{M2} = \frac{1}{2} (v - E_2)q; \\ W = \frac{1}{2} C v^2 + \frac{1}{2} L i_L^2 + \frac{1}{2} (a + 3b\varphi^2)(v - E_1)\varphi + \frac{1}{2} (v - E_2)q; \end{cases} \quad (2)$$

An equivalent Hamilton energy function H in dimensionless form can be obtained by

$$\begin{aligned} H &= \frac{W}{C V_0^2} = \frac{1}{C V_0^2} \left[\frac{1}{2} C v^2 + \frac{1}{2} L i_L^2 + \frac{1}{2} (a + 3b\varphi^2)(v - E_1)\varphi + \frac{1}{2} (v - E_2)q \right] \\ &= \frac{W}{W_0} = \frac{1}{2} x^2 + \frac{1}{2\alpha} y^2 + \frac{1}{2} (a' + b'z^2)(x - e_1)z + \frac{1}{2} (x - e_2)w; \end{aligned} \quad (3)$$

As a result, any changes of the variables and memristive parameters will trigger shift of energy level, and energy is shunted between capacitive, inductive and memristive types. The normalized parameters and dimensionless variables for physical variables and intrinsic parameters are defined by

$$\begin{cases} x = \frac{v}{V_0}, y = \frac{\rho i_L}{V_0}, z = \frac{\varphi}{\rho C V_0}, w = \frac{q}{C V_0}, \tau = \frac{t}{\rho C}, \\ \alpha = \frac{\rho^2 C}{L}, \xi = \frac{R}{\rho}, \\ a' = \rho a, b' = 3b\rho^3 C^2 V_0^2, W_0 = C V_0^2, e = \frac{E}{V_0}, \\ e_1 = \frac{E_1}{V_0}, e_2 = \frac{E_2}{V_0}; \end{cases} \quad (4)$$

According to Eq. (3), the neuron shows jump between energy levels when the electric activities are switched from periodical, spiking, bursting to chaotic patterns. The memristive oscillator regulates its energy value close to certain energy level in presenting sole firing mode. In presence of multiple firing modes, energy level is switched with time. External stimulus can inject energy flux and external electromagnetic field can change the energy shunting between the capacitive and inductive channels, and it explains the mode transition in excitable media under continuous polarization and magnetization.

The circuit equation for Fig. 1 can be obtained as follows

$$\begin{cases} C \frac{dv}{dt} = i_s - i_L - i_{M1} - i_{M2} - i_{NR}; \\ L \frac{di_L}{dt} = v + E - R i_L; \\ \frac{d\varphi}{dt} = v - E_1; \\ \frac{dq}{dt} = i_{M2} = (c + dq^2)(v - E_2); \end{cases} \quad (5)$$

Indeed, the dynamics of the neuron with double memristive channels can be described by equivalent and dimensionless form as follows

$$\begin{cases} \frac{dx}{d\tau} = i'_s - y - (a' + b'z^2)(x - e_1) \\ \quad - (c' + d'w^2)(x - e_2) + x - \frac{1}{2}x^2 - \frac{1}{3}x^3; \\ \frac{dy}{d\tau} = \alpha(x - \xi y + e); \\ \frac{dz}{d\tau} = x - e_1; \\ \frac{dw}{d\tau} = (c' + d'w^2)(x - e_2); \end{cases} \quad (6)$$

By applying and taming the normalized parameters and external forcing current, the firing mode and patterns in the memristive oscillator in Eq. (6) can be

controlled effectively. From Eq. (5) to Eq. (6), scale transformation Eq. (4) is required, and additive scale transformation is used as follows

$$i'_s = \frac{\rho i_s}{V_0}, \quad \zeta = \frac{\rho}{R}, \quad e = \frac{E}{V_0}, \quad c' = \rho c, \quad d' = \rho d C^2 V_0^2; \quad (7)$$

The neural circuit contains magnetic field and electric field energy, and its dynamics can be replaced by equivalent vector form. According to the Helmholtz theorem [39, 40], the solution for the Hamilton energy H of generic nonlinear oscillator in vector form and its derivative of time meets the criterion as follows

$$\begin{cases} \frac{dX}{d\tau} = F_c(X) + F_d(X), \quad X \subset R^n; \\ \nabla H^T F_c(X) = 0; \\ \nabla H^T F_d(X) = \frac{dH}{d\tau}; \end{cases} \quad (8)$$

The physical field is composed of gradient term $F_d(X)$ and curl field term $F_c(X)$, which corresponds to the electric field in the capacitor and magnetic field in inductor of nonlinear circuit, respectively. By the way, the memristive system in Eq. (6) is updated for getting suitable Hamilton energy function, see appendix. An identical energy function as the form in Eq. (3) can be obtained to confirm the reliability of this scheme. The memristive oscillator in Eq. (6) can be approached by discrete form with suitable time step, which is considered as scale parameter ε , and it is defined by

$$\begin{cases} x_{n+1} = x_n + \varepsilon [i'_s - y_n - (a' + b'z_n^2)(x_n - e_1) \\ \quad - (c' + d'w_n^2)(x_n - e_2) + x_n - \frac{1}{2}x_n^2 - \frac{1}{3}x_n^3]; \\ y_{n+1} = y_n + \varepsilon \alpha (x_n - \zeta y_n + e); \\ z_{n+1} = z_n + \varepsilon (x_n - e_1); \\ w_{n+1} = w_n + \varepsilon (c' + d'w_n^2)(x_n - e_2); \end{cases} \quad (9)$$

In addition, the energy function in discrete form is updated as follows

$$H_n = \varepsilon \left[\frac{1}{2}x_n^2 + \frac{1}{2\alpha}y_n^2 + \frac{1}{2}(a' + b'z_n^2)(x_n - e_1)z_n + \frac{1}{2}(x_n - e_2)w_n \right]; \quad (10)$$

The scale parameter ε has similar role as the time step to discretize memristive oscillator presenting in differential equations into a simple map, and its value can be detected by matching the maximal value for

variable x in Eq. (6) and x_n in Eq. (9). That is, all the corresponding parameters are selected the same value, and the scale parameter ε is changed carefully until the two systems cover the same region and maximal value in the phase space. That is, introducing suitable value for the scale parameter ε , the memristive oscillator in Eq. (6) and memristive map in Eq. (9) should have the same dynamical properties including attractors, attraction domain, maximal Lyapunov exponent and same size of phase portrait. When it is considered as a memristive neuron, both of them can present complete spiking, bursting and even chaotic patterns. In this way, the energy function in Eq. (10) with suitable value for ε can measure the energy level for memristive neuron in the form of map. In particular, the memristive map will keep low energy level than the memristive oscillator because the scale parameter ε is often selected with low value ($\varepsilon < 1$). In practical way, memristive map requires low energy than memristive oscillator in signal processing and showing the same dynamical properties. It is important to clarify the approach of energy for some maps by developing equivalent oscillator model so that Helmholtz theorem can be applied for theoretical analysis and prediction for the energy function under periodic stimulus $i'_s = I_0 + A \cos(\omega\tau)$.

It is interesting to discuss the scheme for energy approach for Eqs. (6) and (9) by setting the same group of parameters as $a = 0.01$, $b = 0.01$, $c = 0.01$, $d = 0.01$, $e = 0.05$, $e_1 = 0.05$, $e_2 = 0.06$, $\alpha = 1.21$; $\zeta = 0.15$, $A = 1.0$, $I_0 = 0.9$, and same initials setting are selected for the variables $(x, y, z, w) = (x_n, y_n, z_n, w_n) = (0.2, 0.1, 0.01, 0.01)$. The bifurcation analysis and average energy are plotted in Fig. 2.

The firing mode, profile of attractors and average energy of the memristive neuron will be controlled by external stimulus with changing the angular frequency. To confirm the consistence and similarity of attractors and firing patterns between the memristive neuron and map, scale parameter is adjusted to track the maximal value for membrane potential and average energy in Fig. 3.

From Fig. 3, the memristive neuron in Eq. (6) can be reproduced the same firing patterns and attractors in the memristive map in Eq. (9) by setting suitable value for scale parameter ε . The energy level and firing mode in the neuron in Eq. (6) are dependent on the angular frequency of external stimulus. From Eqs. (3)–(10), the discrete neuron is endowed with scale parameter ε ,

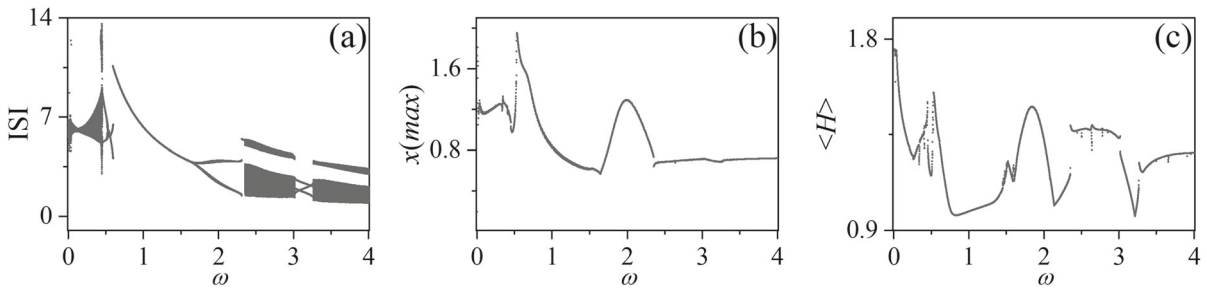


Fig. 2 Bifurcation of ISI (interspike interval) from membrane potential, $x_{max} = x(max)$ for maximal value of membrane potential, and average Hamilton energy $\langle H \rangle$ with changing frequency ω in Eq. (6)

as a result, its average energy $\langle H_n \rangle$ becomes less than $\langle H \rangle$ because $\epsilon < 1$. Therefore, it is suitable to reproduce similar firing patterns and attractors of nonlinear oscillators in some equivalent maps by setting appropriate value for the scale parameter when they are selected with the same parameters. Particularly, the energy level in the equivalent map is decreased greatly than the memristive oscillator. In a word, scale parameter can be introduced into the discrete energy function for the equivalent map reduced from the memristive oscillator with the same parameters setting. It is important to calculate the energy function for a memristive map by developing similar memristive oscillator, and then the energy function will be discretized by removing the scale parameter directly.

3 Energy descriptions in memristive map

From dynamical viewpoint, discrete systems and maps can be considered as discretized forms for continuous dynamical systems by applying Euler algorithm approach with suitable time step. For a generic dynamical system expressed by differential equations,

$$\begin{cases} \frac{dx}{d\tau} = f(x, y, z); \\ \frac{dy}{d\tau} = g(x, y, z); \\ \frac{dz}{d\tau} = h(x, y, z); \end{cases} \tag{11}$$

Its equivalent discrete form is obtained by

$$\begin{cases} x_{n+1} = x_n + \epsilon f(x_n, y_n, z_n); \\ y_{n+1} = y_n + \epsilon g(x_n, y_n, z_n); \\ z_{n+1} = z_n + \epsilon h(x_n, y_n, z_n); \end{cases} \tag{12}$$

where the parameter ϵ denotes the time scale, Eq. (12) will match with Eq. (11) in dynamical characteristic by setting suitable values for ϵ . Based on Helmholtz theorem, the Hamilton energy function for dynamical systems similar to Eq. (11) can be obtained theoretically. From Eq. (3), the continuous energy function is dependent on some intrinsic parameters and all the variables in the memristive system, and any changes in the firing patterns will induce fluctuations in the energy levels. For discrete systems, energy function becomes discrete as well. Indeed, appropriate scale parameter with time can be applied to convert discrete systems into equivalent continuous system for obtaining energy function.

$$\begin{cases} x_{n+1} = F(x_n, y_n, z_n); \\ y_{n+1} = G(x_n, y_n, z_n); \\ z_{n+1} = W(x_n, y_n, z_n); \end{cases} \Rightarrow \begin{cases} \frac{1}{\epsilon} [x_{n+1} - x_n] = \frac{1}{\epsilon} [F(x_n, y_n, z_n) - x_n]; \\ \frac{1}{\epsilon} [y_{n+1} - y_n] = \frac{1}{\epsilon} [G(x_n, y_n, z_n) - y_n]; \\ \frac{1}{\epsilon} [z_{n+1} - z_n] = \frac{1}{\epsilon} [W(x_n, y_n, z_n) - z_n]; \end{cases}$$

$$\Rightarrow \begin{cases} \frac{dx}{d\tau} = \frac{1}{\epsilon} [F(x, y, z) - x]; \\ \frac{dy}{d\tau} = \frac{1}{\epsilon} [G(x, y, z) - y]; \\ \frac{dz}{d\tau} = \frac{1}{\epsilon} [W(x, y, z) - z]; \end{cases} \tag{13}$$

According to the criterion in Eq. (8), the Hamilton energy for the discrete system in Eq. (13) can be expressed in generic form

$$\begin{cases} H = H(\epsilon, x, y, z); \\ H_n = H(x_n, y_n, z_n); \end{cases} \tag{14}$$

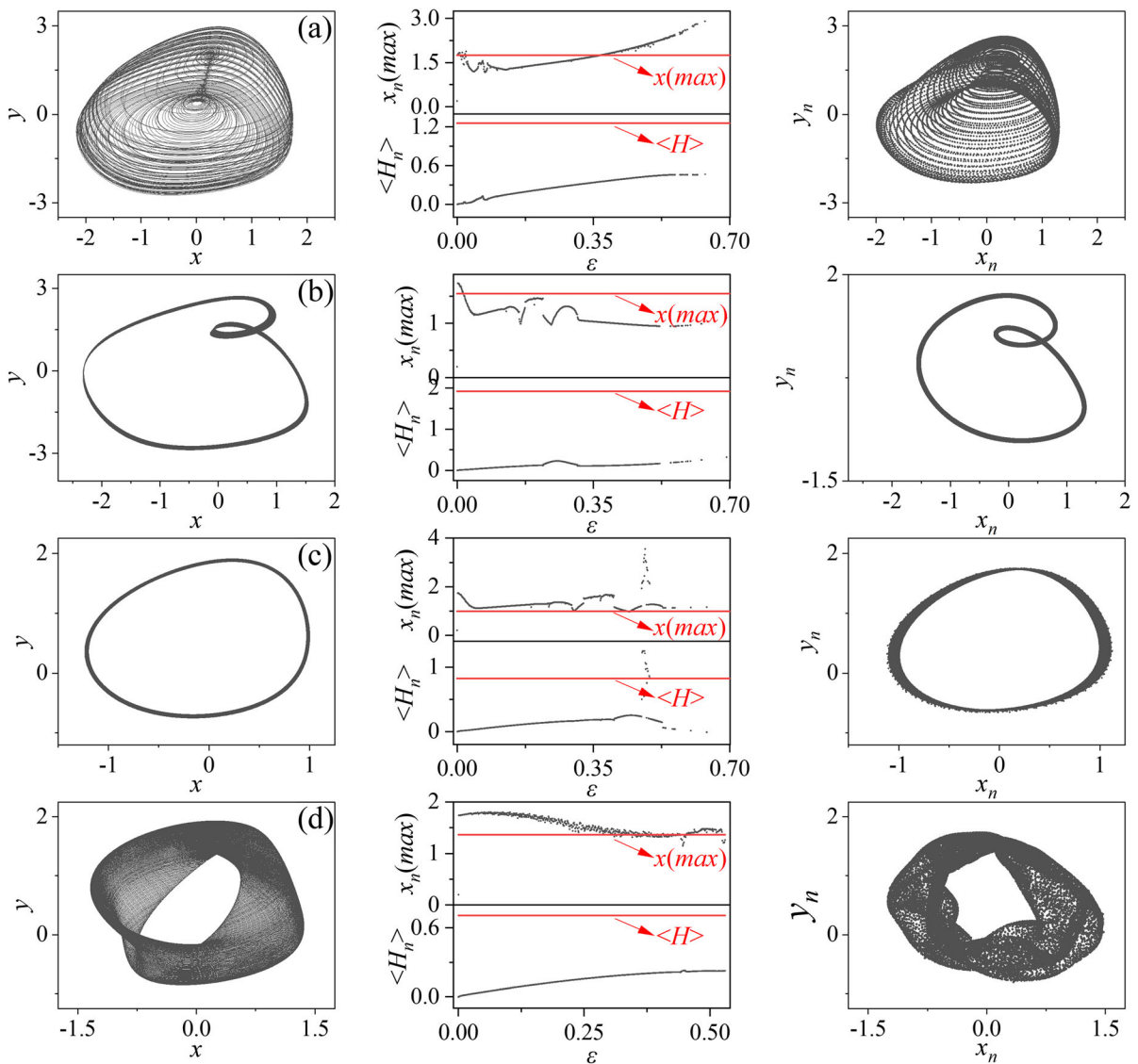


Fig. 3 Different attractors for the memristive neuron/map in Eqs. (6) and (9) under suitable scale parameter ϵ , and the average energy $\langle H_n \rangle$ and $x_n(max)$ in memristive discrete neuron via

scale parameter ϵ . For **a** bursting $\omega = 0.035$, $\epsilon = 0.104$; **b** spiking $\omega = 0.53$, $\epsilon = 0.29$; **c** periodic $\omega = 1.0$, $\epsilon = 0.0013$; **d** chaotic $\omega = 2.9$, $\epsilon = 0.5$

For a memristive map developed from Hénon map,

$$\begin{cases} x_{n+1} = 1 + by_n - ax_n^2 - (\alpha + 3\beta\varphi_n^2)x_n; \\ y_{n+1} = x_n; \\ \varphi_{n+1} = \varphi_n + cx_n; \end{cases} \quad (15)$$

By introducing appropriate scale parameter, it obtains equivalent memristive oscillator as follows

$$\begin{cases} \frac{dx}{d\tau} = \frac{1}{\epsilon} [1 + by - ax^2 - (\alpha + 1 + 3\beta\varphi^2)x]; \\ \frac{dy}{d\tau} = \frac{1}{\epsilon} (x - y); \\ \frac{d\varphi}{d\tau} = \frac{c}{\epsilon} x; \end{cases} \quad (16)$$

From dynamical viewpoint, appropriate setting for the scale parameter in Eq. (16) will reproduce similar dynamical characteristic as in Eq. (15) under setting the same parameters. In practical way, appropriate

electric components can be combined to reproduce similar signals in the analog circuit by applying suitable physical parameters for these potential electric components. Based on the Helmholtz theorem, the energy function for Eq. (16) can be defined and obtained in theoretical way. It can be expressed in the vector form containing two kinds of physical fields as follows

$$\begin{aligned}
 \begin{pmatrix} \dot{x} \\ \dot{y} \\ \dot{\varphi} \end{pmatrix} &= F_c + F_d = \begin{pmatrix} -\frac{by}{\varepsilon} - \frac{bc}{2\varepsilon}(\alpha + 3\beta\varphi^2)x \\ \frac{x}{\varepsilon} - \frac{1}{\varepsilon}b\beta\varphi^3 \\ \frac{cx}{\varepsilon} + \frac{b\varphi y}{\varepsilon x} + \frac{bc}{2\varepsilon}(\alpha\varphi + \beta\varphi^3) \end{pmatrix} \\
 &+ \begin{pmatrix} \frac{1}{\varepsilon}[1 + 2by - ax^2 - (\alpha + 1 + 3\beta\varphi^2)x + \frac{bc}{2}(\alpha + 3\beta\varphi^2)x] \\ -\frac{y}{\varepsilon} + \frac{1}{\varepsilon}b\beta\varphi^3 \\ -\frac{b\varphi y}{\varepsilon x} - \frac{bc}{2\varepsilon}(\alpha\varphi + \beta\varphi^3) \end{pmatrix} \\
 &= \begin{pmatrix} 0 & -b & -bc \\ b & 0 & -\frac{b\varphi}{x} \\ bc & \frac{b\varphi}{x} & 0 \end{pmatrix} \begin{pmatrix} \frac{x}{\varepsilon b} + \frac{1}{2\varepsilon}(\alpha\varphi + \beta\varphi^3) \\ \frac{y}{\varepsilon} \\ \frac{x}{2\varepsilon}(\alpha + 3\beta\varphi^2) \end{pmatrix} \\
 &+ \begin{pmatrix} A_{11} & 0 & 0 \\ 0 & A_{22} & 0 \\ 0 & 0 & A_{33} \end{pmatrix} \begin{pmatrix} \frac{x}{\varepsilon b} + \frac{1}{2\varepsilon}(\alpha\varphi + \beta\varphi^3) \\ \frac{y}{\varepsilon} \\ \frac{x}{2\varepsilon}(\alpha + 3\beta\varphi^2) \end{pmatrix}; \tag{17}
 \end{aligned}$$

The coefficient for the matrix in Eq. (17) is defined by

$$\begin{cases} A_{11} = \frac{1 - ax^2 - (\alpha + 1 + 3\beta\varphi^2)x + \frac{bc}{2}(\alpha + 3\beta\varphi^2)x}{\frac{1}{b}x + \frac{1}{2}(\alpha\varphi + \beta\varphi^3)}; \\ A_{22} = \frac{-y + \beta\varphi^3}{y}; \quad A_{33} = \frac{-\frac{2b\varphi y}{x} - bc(\alpha\varphi + \beta\varphi^3)}{(\alpha + 3\beta\varphi^2)x}; \end{cases} \tag{18}$$

The solution for Hamilton energy function can be suggested as follows

$$H = \frac{1}{\varepsilon} \left[\frac{1}{2b}x^2 + \frac{1}{2}y^2 + \frac{1}{2}(\alpha\varphi + \beta\varphi^3)x \right]; \tag{19}$$

As a result, the discrete energy function for Eq. (15) is updated by

$$\begin{aligned}
 H_n &= H_1 + H_2 + H_M \\
 &= \frac{1}{2b}x_n^2 + \frac{1}{2}y_n^2 + \frac{1}{2}(\alpha\varphi_n + \beta\varphi_n^3)x_n; \tag{20}
 \end{aligned}$$

Compared to Eq. (15), and additive scale parameter ε is introduced into Eq. (16), bifurcation analysis can be applied to detect the region for ε when other parameters are fixed the same setting for the memristive map in Eq. (15). Three terms including H_1, H_2 and H_M mark the capacitive, inductive energy and memristive energy, respectively. To cover the same phase space, the parameter ε is changed from 0.001 to a finite threshold, and the maximal value (x_{max}) for the variable x is selected to match the maximal value $x_{max}(n)$ and then the suitable value for parameter ε will be confirmed. By taming the value for the scale parameter ε , the dynamics of the memristive map in Eq. (15) will be reproduced by memristive oscillator in Eq. (16) completely by showing the same attractor, sampled time series, maximal Lyapunov exponent, size of phase portrait in the phase space. In simple way, both the continuous and discrete systems have the same maximal value for the first variables, and it can be confirmed via bifurcation analysis with changing the parameter ε carefully. As a result, the energy function in Eq. (19) with exact parameter ε will address the energy property for the memristive map in Eq. (15) well.

In fact, there are three terms for energy sources kept in certain channels or components, and the oscillatory state is dependent on the energy shunting between these channels. Any changes of parameters in Eq. (15) will modify the oscillatory mode and the energy level in Eq. (20) will be adjusted synchronously. As a result, energy ration between the three terms will be adjusted when oscillation is changed. The energy ratio is defined in

$$\begin{cases} p_1 = \frac{H_1}{H_n} = \frac{\frac{1}{2b}x_n^2}{\frac{1}{2b}x_n^2 + \frac{1}{2}y_n^2 + \frac{1}{2}(\alpha\varphi_n + \beta\varphi_n^3)x_n}; \\ p_2 = \frac{H_2}{H_n} = \frac{\frac{1}{2}y_n^2}{\frac{1}{2b}x_n^2 + \frac{1}{2}y_n^2 + \frac{1}{2}(\alpha\varphi_n + \beta\varphi_n^3)x_n}; \\ p_3 = \frac{H_M}{H_n} = \frac{\frac{1}{2}(\alpha\varphi_n + \beta\varphi_n^3)x_n}{\frac{1}{2b}x_n^2 + \frac{1}{2}y_n^2 + \frac{1}{2}(\alpha\varphi_n + \beta\varphi_n^3)x_n}; \end{cases} \tag{21}$$

In fact, H_1 and H_2 can present capacitive and inductive energy, and the ratio $H_1:H_2$ is also effective to predict mode transition in the oscillatory states. Similar energy proportion $P_1=H_1/H, P_2 = (H_2+H_M)/H$ can be

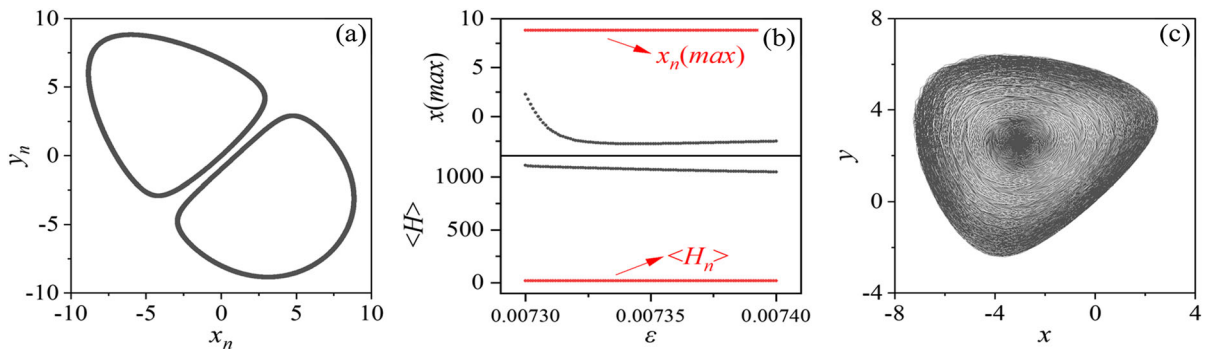


Fig. 4 **a** Attractor in memristive map in Eq. (15); **b** average energy $\langle H \rangle$ and x_{max} versus with scale parameter ε ; **c** chaotic attractor in Eq. (16) at $\varepsilon = 0.0073$. Equations (15) and (16)

defined to estimate the regulation on dynamics from capacitive and inductive energy, respectively. From the memristive map in Eq. (15) and memristive oscillator in Eq. (16), parameters can be adjusted to trigger periodic or chaotic behaviors. The involvement of scale parameter into energy function in Eq. (19) can increase the energy level directly during the conversion from memristive map to nonlinear oscillator. In Fig. 4, parameters are selected to develop chaotic attractors in the memristive map, and the same parameters and suitable scale parameter are endowed to mimic the oscillatory characteristic in the memristive map. The scale parameter is also adjusted to track the evolution of the average energy and maximal value for the variable x in the memristive oscillator in Eq. (16) as well.

Two chaotic rings are formed in the phase space for the memristive map, while chaotic attractors are induced in the memristive oscillator in Eq. (16) by taming the scale parameter $\varepsilon=0.0073$. The maximal value for the memristive map and memristive oscillator has similar oscillation, while their average energy has distinct diversity because of the involvement of scale parameter. Indeed, the scale parameter is adjusted carefully but the maximal values still show some difference even they can present similar oscillatory characteristic with time. It indicates that the

select the same parameters as $b = 1.0$, $a = 0.05$, $\alpha = 0$, $\beta = 0$, $c = 0.1$; initials $(x, y, \varphi) = (x_n, y_n, \varphi_n) = (0.02, 0.01, 0.01)$

memristive oscillator has no bridge to potential equivalent nonlinear circuits.

On the other hand, the same parameters setting for memristive map in Eq. (15) and memristive oscillator in Eq. (16) can be applied, the scale parameter ε can be adjusted to keep them in same energy level as $H=H_n$ synchronously even they can present different attractors and firing patterns. In fact, the weight for each energy term is crucial for selecting the firing patterns and mode, and the introduction of scale parameter ε seldom changes the energy proportion among the capacitive, inductive and memristive energy terms. In this way, most of the maps can be updated with equivalent oscillators, which the corresponding Hamilton energy functions are obtained by using Helmholtz theorem, the suitable energy function for the maps can be obtained by removing the scale parameters for the Hamilton energy function for the nonlinear oscillators. In Fig. 5, the scale parameter is adjusted to keep the memristive map and memristive oscillator with the same energy level by changing the scale parameter carefully and parameters for the two memristive systems are different.

When the memristive map and memristive oscillator are endowed with different parameters setting, appropriate selection of scale parameter can ensure two memristive systems keep the same energy level and same oscillatory state. In fact, the Hamilton

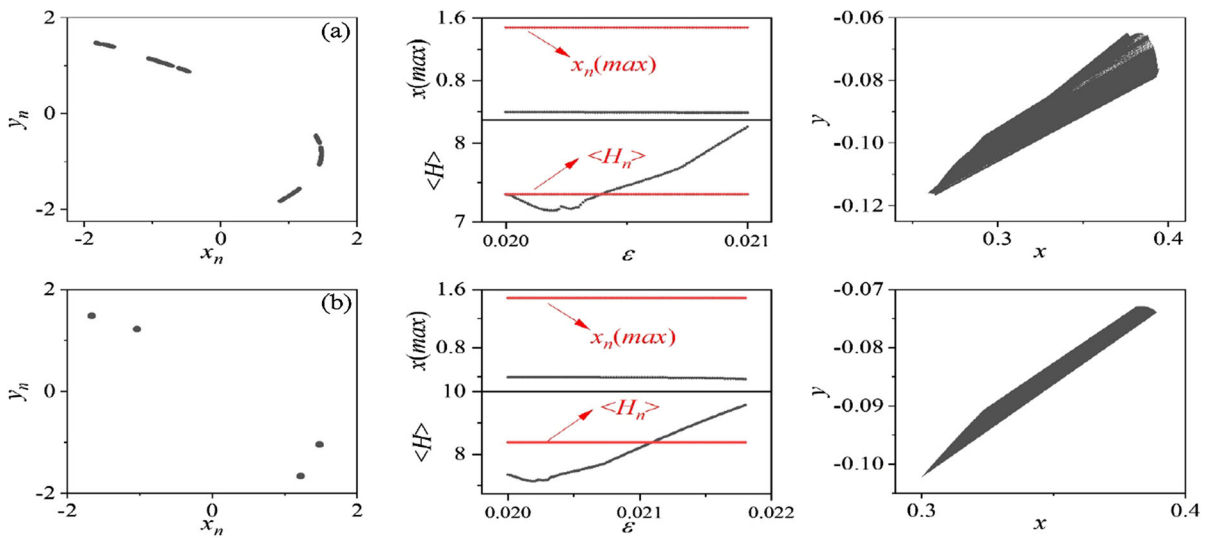


Fig. 5 Attractors in Eqs. (15) and (16) with the same energy level, average energy $\langle H \rangle$ and x_{max} versus under different value for ϵ . For **a** chaotic map, $\beta = 0.002$, $\epsilon = 0.0204$, $\beta' = 0.154$; **b** periodic map, $\beta = 0.08$, $\epsilon = 0.02109$, $\beta' = 0.154$. Setting $b = 0.1$, $a = 0.62$, $\alpha = 0.1$, $\beta = 0.01$,

$c = 0.2$ in Eq. (15); $b' = 0.102$, $a' = 1.725$, $\alpha' = 2.05$, $\beta' = 0.154$, $c' = 0.0009$ in Eq. (16); same initials $(x, y, \varphi) = (x_n, y_n, \varphi_n) = (0.02, 0.01, 0.01)$. In the figures, $x_{max} = x(max)$, $x_n(max)$ denote the maximal value in the sampled time series for two memristive systems

energy function is a kind of Lyapunov function and restricts the cooperation between different variables of the system. For physical oscillators converted from nonlinear circuits, the sole Hamilton energy is derived from the field energy including inductive, capacitive and memristive components. The weight for each term of the energy function is decided by the normalized parameters after scale transformation for all physical variables and parameters. As a result, these weights are more important in the energy function than the scale parameter. From a nonlinear oscillator to a map, continuous energy function is replaced by discrete energy function with suitable scale parameter. From a map to a continuous oscillator, the weight for each energy term can be confirmed and energy function for the map has no scale parameter, but the discrete energy function is helpful to predict the mode transition accompanying with shift in energy level.

From physical viewpoint, most of the nonlinear oscillators in mathematical form can be derived from equivalent circuit equations and mechanical systems. The activation and exchange of energy flow are

dominated by the physical properties of physical elements, which also govern the nonlinear terms in the dynamical equations and mathematical models. For most of the nonlinear circuits, the field energy can be obtained by summing the energy in each electric component, and they can be converted into dimensionless energy function after scale transformation. For generic nonlinear oscillators, the application of Helmholtz theorem provides help to get the Hamilton energy function, which is considered as a kind of Lyapunov function, and specific terms for energy terms means special electric components should be used in this circuit. Memristor is a functional electric competent, and its memristive properties throw lights for activating self-adaptive property of nonlinear terms in the physical systems and network, and energy flow can be controlled in adaptive way in presence of external field. As a result, the involvement of memristive term into dynamical systems can explain the self-controllability and adaption greatly [41–43]. Energy characteristic of nervous and neural circuits is very important [44], and physical energy in neural

circuits can be obtained in theoretical way, which Helmholtz theorem can confirm its correctness when the physical energy is converted into dimensionless Hamilton energy. In experimental way, the transient performances of the circuit should be considered [45] in the realization of analog circuits, and so the reliability of the neural circuits can be verified and evaluated.

For discrete systems and maps, scale parameter is introduced to build an equivalent nonlinear oscillator in the form of ODEs (Ordinary differential equations) and its energy function also contains the same scale parameter. Based on the Helmholtz theorem, energy function for the nonlinear oscillator is obtained and then it is discretized to denote the energy function without scale parameter for the map. In the phase space, the nonlinear oscillator will cover the same phase size and maximal value as the map when the scale parameter is adjusted carefully. For some specific maps defined in mathematical form, there are some differences in the maximal value for variables in the map and nonlinear oscillator. Referring to the energy characteristic of the known electric components, the generic form of the Hamilton energy function can be suggested, and scale parameter is introduced to confirm its exact value when the nonlinear oscillator model matches with the map in phase space completely. The scheme can be further used to explore the formation of defects and heterogeneity [46, 47] in discrete networks when energy function for each node is estimated exactly.

For obtaining exact energy function for generic maps, equivalent nonlinear oscillators can be designed by defining appropriate transformation for the parameters and discrete variables as follows.

$$\begin{cases} x_{n+1} = f(x_n, \lambda) \Rightarrow \frac{dy}{d\tau} = f(y, p), y = \{y_1, y_2, \dots, y_n, \dots\}; \\ \lambda = \lambda(p, h), x_n = x_n(y_n, h, p); \text{ or} \\ p = p(\lambda, h), y_n = y_n(x_n, h, \lambda); h \text{ is time step} \end{cases} \quad (22)$$

where the map and continuous oscillator has the same local kinetics but the parameters and variables have certain relevance, that is, the parameter p differs from λ for presenting the same dynamics. For

example, the Logistic map can be described by a Logistic oscillator by using the transformation in Eq. (22) [48].

4 Conclusions

In this work, field energy for a memristor-coupled circuit is defined and its equivalent dimensionless Hamilton energy for the memristive oscillator is obtained by applying scale transformation. The approach of energy function is also confirmed by using Helmholtz theorem. The memristive oscillator is reduced into discrete map and its equivalent energy form is obtained by setting suitable scale parameter. Keeping the same dynamical characteristics, memristive map shows lower energy level than the memristive oscillator. In addition, a memristive map developed from Hénon map added with memristive term is integrated into equivalent continuous oscillator by introducing suitable scale parameter, and its energy function is approached in theoretical way. Furthermore, discrete energy function is confirmed to describe the energy characteristic of the memristive Hénon map. This scheme can be further used to estimate the energy function for other discrete systems even discrete memristor is coupled. That is, maps are updated with equivalent nonlinear oscillators for getting theoretical energy function with scale parameter, and the generic energy function for the map can be obtained by removing the scale parameter for the energy function of its equivalent nonlinear oscillator.

Acknowledgements This project is supported by the National Natural Science Foundation of China under Grant Nos. 12072139.

Funding The authors have not disclosed any funding.

Data availability The data are available upon reasonable request.

Declarations

Conflict of interest The authors declare that they have no conflict of interest with this publication.

Appendix

$$\begin{cases} A_{11} = \frac{i'_s + (a' + b'z^2)(x - e_1) - (c' + d'w^2)(x - e_2) + x - \frac{1}{2}x^2 - \frac{1}{3}x^3 + \frac{1}{2}(x - e_1)(a' + 3b'z^2) + \frac{1}{2}c'(x - e_2)}{x + \frac{1}{2}(a'z + b'z^3) + \frac{1}{2}w} \\ A_{22} = \frac{\alpha^2[e - \zeta y - \frac{1}{2}(a'z + b'z^3) - \frac{1}{2}w - \frac{3b'}{2a'}z^2(x - e_1) - \frac{1}{2}(e_2 - e_1)]}{-2e_1 - (a'z + b'z^3) - w + 2\frac{y}{a'}} \\ A_{33} = \frac{(x - e_1)(a' + 3b'z^2)}{-2c'e_2 + 2d'w^2(x - e_2) - c'(a'z + b'z^3) - c'w - 2y} \\ A_{44} = \frac{(x - e_2)}{(x - e_2)} \end{cases} \tag{A1}$$

$$\begin{pmatrix} \dot{x} \\ \dot{y} \\ \dot{z} \\ \dot{w} \end{pmatrix} = F_c + F_d = \begin{pmatrix} -y - \frac{1}{2}(x - e_1)(a' + 3b'z^2) - \frac{1}{2}c'(x - e_2) \\ \alpha x + \frac{1}{2}\alpha(a'z + b'z^3) + \frac{1}{2}\alpha w + \frac{3\alpha b'}{2a'}z^2(x - e_1) + \frac{1}{2}\alpha(e_2 - e_1) \\ x + \frac{1}{2}(a'z + b'z^3) + \frac{1}{2}w - \frac{y}{a'} \\ c'x + \frac{1}{2}c'a'z + b'z^3 + \frac{1}{2}c'w + y \end{pmatrix} \\ + \begin{pmatrix} i'_s + (a' + b'z^2)(x - e_1) - (c' + d'w^2)(x - e_2) + x - \frac{1}{2}x^2 - \frac{1}{3}x^3 + \frac{1}{2}(x - e_1)(a' + 3b'z^2) + \frac{1}{2}c'(x - e_2) \\ \alpha e - \alpha\zeta y - \frac{1}{2}\alpha(a'z + b'z^3) - \frac{1}{2}\alpha w - \frac{3\alpha b'}{2a'}z^2(x - e_1) - \frac{1}{2}\alpha(e_2 - e_1) \\ -e_1 - \frac{1}{2}(a'z + b'z^3) - \frac{1}{2}w + \frac{y}{a'} \\ -c'e_2 + d'w^2(x - e_2) - \frac{1}{2}c'(a'z + b'z^3) - \frac{1}{2}c'w - y \end{pmatrix}; \\ = \begin{pmatrix} 0 & -\alpha & -1 & -c' \\ \alpha & 0 & \frac{\alpha}{a'} & -\alpha \\ 1 & -\frac{\alpha}{a'} & 0 & 0 \\ c' & \alpha & 0 & 0 \end{pmatrix} \begin{pmatrix} x + \frac{1}{2}(a'z + b'z^3) + \frac{1}{2}w \\ \frac{y}{\alpha} \\ \frac{1}{2}(x - e_1)(a' + 3b'z^2) \\ \frac{1}{2}(x - e_2) \end{pmatrix} + \begin{pmatrix} A_{11} & 0 & 0 & 0 \\ 0 & A_{22} & 0 & 0 \\ 0 & 0 & A_{33} & 0 \\ 0 & 0 & 0 & A_{44} \end{pmatrix} \begin{pmatrix} x + \frac{1}{2}(a'z + b'z^3) + \frac{1}{2}w \\ \frac{y}{\alpha} \\ \frac{1}{2}(x - e_1)(a' + 3b'z^2) \\ \frac{1}{2}(x - e_2) \end{pmatrix}; \tag{A2}$$

References

1. Kavehei, O., Iqbal, A., Kim, Y.S., et al.: The fourth element: characteristics, modelling and electromagnetic theory of the memristor. *Proc. Royal Soc. A: Math. Phys. Eng. Sci.* **466**, 2175–2202 (2010)
2. Yeşil, A., Babacan, Y., Kaçar, F.: A new DDCC based memristor emulator circuit and its applications. *Microelectron. J.* **45**, 282–287 (2014)
3. Zidan, M.A., Fahmy, H.A.H., Hussain, M.M., et al.: Memristor-based memory: the sneak paths problem and solutions. *Microelectron. J.* **44**, 176–183 (2013)
4. Wang, L., Yang, C.H., Wen, J., et al.: Overview of emerging memristor families from resistive memristor to spintronic memristor. *J. Mater. Sci.: Mater. Electron.* **26**, 4618–4628 (2015)
5. Goswami, S., Pramanick, R., Patra, A., et al.: Decision trees within a molecular memristor. *Nature* **597**, 51–56 (2021)
6. Kuznetsov, N., Mokaev, T., Ponomarenko, V., et al.: Hidden attractors in Chua circuit: mathematical theory meets physical experiments. *Nonlinear Dyn.* **111**, 5859–5887 (2023)
7. Wang, E., Yan, S., Sun, X., et al.: Analysis of bifurcation mechanism of new hyperchaotic system, circuit

- implementation, and synchronization. *Nonlinear Dyn.* **111**, 3869–3885 (2023)
8. Vijay, S.D., Thamilmaran, K., Ahamed, A.I.: Superextreme spiking oscillations and multistability in a memristor-based Hindmarsh-Rose neuron model. *Nonlinear Dyn.* **111**, 789–799 (2023)
 9. Xu, H., Zhang, Z., Peng, M.: Novel bursting patterns and the bifurcation mechanism in a piecewise smooth Chua's circuit with two scales. *Nonlinear Dyn.* **108**, 1755–1771 (2022)
 10. Zhang, X., Ma, J.: Wave filtering and firing modes in a light-sensitive neural circuit. *J. Zhejiang Univ. Sci. A* **9**, 707–720 (2021)
 11. Guan, M.J., Liao, W.H.: On the equivalent circuit models of piezoelectric ceramics. *Ferroelectrics* **386**, 77–87 (2009)
 12. Karthikeyan, A., Cimen, M.E., Akgul, A., et al.: Persistence and coexistence of infinite attractors in a fractal Josephson junction resonator with unharmonic current phase relation considering feedback flux effect. *Nonlinear Dyn.* **103**, 1979–1998 (2021)
 13. Zhang, Y., Xu, Y., Yao, Z., et al.: A feasible neuron for estimating the magnetic field effect. *Nonlinear Dyn.* **102**, 1849–1867 (2020)
 14. Xie, Y., Yao, Z., Hu, X., et al.: Enhance sensitivity to illumination and synchronization in light-dependent neurons. *Chin. Phys. B* **30**, 120510 (2021)
 15. Liu, Y., Xu, W., Ma, J., et al.: A new photosensitive neuron model and its dynamics. *Front. Informa. Technol. Electron. Eng.* **21**, 1387–1396 (2020)
 16. Ibrahim, O., Hassan, S.M., Abdulkarim, A., et al.: Design of wheatstone bridge based thermistor signal conditioning circuit for temperature measurement. *J. Eng. Sci. Technol. Rev.* **12**, 12–17 (2019)
 17. Naveen Kumar, V., Lakshmi Narayana, K.V.: Development of thermistor signal conditioning circuit using artificial neural networks. *IET Sci. Meas. Technol.* **9**, 955–961 (2015)
 18. Groschner, L.N., Malis, J.G., Zuidinga, B., et al.: A biophysical account of multiplication by a single neuron. *Nature* **603**, 119–123 (2022)
 19. Ma, J.: Biophysical neurons, energy, and synapse controllability: a review. *J. Zhejiang Univ. Sci. A* **24**, 109–129 (2023)
 20. Wu, F., Hu, X., Ma, J.: Estimation of the effect of magnetic field on a memristive neuron. *Appl. Math. Comput.* **432**, 127366 (2022)
 21. Wu, F., Ma, J., Zhang, G.: A new neuron model under electromagnetic field. *Appl. Math. Comput.* **347**, 590–599 (2019)
 22. Di Maio, V., Santillo, S., Ventriglia, F.: Synaptic dendritic activity modulates the single synaptic event. *Cogn. Neurodyn.* **15**, 279–297 (2021)
 23. Wang, C., Yao, Z., Xu, W., et al.: Phase synchronization between nonlinear circuits by capturing electromagnetic field energy. *Mod. Phys. Lett. B* **34**, 2050323 (2020)
 24. Zhou, P., Ma, J., Tang, J.: Clarify the physical process for fractional dynamical systems. *Nonlinear Dyn.* **100**, 2353–2364 (2020)
 25. Zhou, P., Zhang, X., Hu, X., et al.: Energy balance between two thermosensitive circuits under field coupling. *Nonlinear Dyn.* **110**, 1879–1895 (2022)
 26. Ren, L., Lin, M.H., Abdulwahab, A., et al.: Global dynamical analysis of the integer and fractional 4D hyperchaotic Rabinovich system. *Chaos, Solit. Fract.* **169**, 113275 (2023)
 27. Leutcho, G.D., Khalaf, A.J.M., Njitacke Tabekoueng, Z., et al.: A new oscillator with mega-stability and its Hamilton energy: infinite coexisting hidden and self-excited attractors. *Chaos* **30**, 033112 (2020)
 28. Njitacke, Z.T., Takembo, C.N., Awrejcewicz, J., et al.: Hamilton energy, complex dynamical analysis and information patterns of a new memristive FitzHugh-Nagumo neural network. *Chaos, Solit. Fract.* **160**, 112211 (2022)
 29. Rong, K., Bao, H., Li, H., et al.: Memristive Hénon map with hidden Neimark-Sacker bifurcations. *Nonlinear Dyn.* **108**, 4459–4470 (2022)
 30. Peng, Y., Sun, K., He, S.: A discrete memristor model and its application in Hénon map. *Chaos, Solitons Fractals* **137**, 109873 (2020)
 31. Fouda, M.E., Radwan, A.G.: Charge controlled memristor-less memcapacitor emulator. *Electron. Lett.* **48**, 1454–1455 (2012)
 32. Petrović, P.B.: Charge-controlled grounded memristor emulator circuits based on Arbel-Goldminz cell with variable switching behaviour. *Analog Integr. Circ. Sig. Process* **113**, 373–381 (2022)
 33. Yang, F., Xu, Y., Ma, J.: A memristive neuron and its adaptability to external electric field. *Chaos* **33**, 023110 (2023)
 34. Lin, R., Shi, G., Qiao, F., et al.: Research progress and applications of memristor emulator circuits. *Microelectron. J.* **133**, 105702 (2023)
 35. Yao, Z., Zhou, P., Alsaedi, A., et al.: Energy flow-guided synchronization between chaotic circuits. *Appl. Math. Comput.* **374**, 124998 (2020)
 36. Bao, B., Hu, J., Cai, J., et al.: Memristor-induced mode transitions and extreme multistability in a map-based neuron model. *Nonlinear Dyn.* **111**, 3765–3779 (2023)
 37. Vijayakumar, M.D., Natiq, H., Meli, M.I.T., et al.: Hamiltonian energy computation of a novel memristive megastable oscillator (MMO) with dissipative, conservative and repelled dynamics. *Chaos, Solit. Fract.* **155**, 111765 (2022)
 38. Wang, G., Xu, Y., Ge, M., et al.: Mode transition and energy dependence of FitzHugh-Nagumo neural model driven by high-low frequency electromagnetic radiation. *AEU-Int. J. Electron. Commun.* **120**, 153209 (2020)
 39. Xie, Y., Zhou, P., Ma, J.: Energy balance and synchronization via inductive-coupling in functional neural circuits. *Appl. Math. Model.* **113**, 175–187 (2023)
 40. Kobe, D.H.: Helmholtz's theorem revisited. *Am. J. Phys.* **54**, 552–554 (1986)
 41. Song, F., Liu, Y., Shen, D., et al.: Learning control for motion coordination in wafer scanners: toward gain adaptation. *IEEE Trans. Industr. Electron.* **69**, 13428–13438 (2022)
 42. Zhang, C., Kordestani, H., Shadabfar, M.: A combined review of vibration control strategies for high-speed trains and railway infrastructures: challenges and solutions. *J. Low Freq. Noise Vib. Active Control* **42**, 272–291 (2023)
 43. Li, D., Yu, H., Tee, K.P., et al.: On time-synchronized stability and control. *IEEE Trans. Syst. Man Cyber. Syst.* **52**, 2450–2463 (2021)

44. Wang, R., Wang, Y., Xu, X., et al.: Brain works principle followed by neural information processing: a review of novel brain theory. *Artif. Intell. Rev.* (2023). <https://doi.org/10.1007/s10462-023-10520-5>
45. Xia, C., Zhu, Y., Zhou, S., et al.: Simulation study on transient performance of a marine engine matched with high-pressure SCR system. *Int. J. Engine Res.* **24**, 1327–1345 (2023)
46. Yang, F., Wang, Y., Ma, J.: Creation of heterogeneity or defects in a memristive neural network under energy flow. *Commun. Nonlinear Sci. Numer. Simul.* **119**, 107127 (2023)
47. Xie, Y., Yao, Z., Ma, J.: Formation of local heterogeneity under energy collection in neural networks. *Sci. China Technol. Sci.* **66**, 439–455 (2023)
48. Shen, B. W., Pielke, R. A. Sr, Zeng, X.: The 50th Anniversary of the Metaphorical Butterfly Effect since

Lorenz (1972): Multistability, Multiscale Predictability, and Sensitivity in Numerical Models. *Atmosphere*, 14(8): 1279 (2023)

Publisher's Note Springer Nature remains neutral with regard to jurisdictional claims in published maps and institutional affiliations.

Springer Nature or its licensor (e.g. a society or other partner) holds exclusive rights to this article under a publishing agreement with the author(s) or other rightsholder(s); author self-archiving of the accepted manuscript version of this article is solely governed by the terms of such publishing agreement and applicable law.